The role of excess arsenic in interface mixing in low-temperature-grown AlAs/GaAs superlattices

I. Lahiri[a] and D. D. Nolte
Department of Physics and the MRSEC for Technology-Enabling Heterostructure Materials, Purdue University, West Lafayette, Indiana 47907-1396

J. C. P. Chang, J. M. Woodall, and M. R. Melloch
School of Electrical Engineering and the MRSEC for Technology-Enabling Heterostructure Materials, Purdue University, West Lafayette, Indiana 47907-1285

(Received 27 April 1995; accepted for publication 22 June 1995)

Undoped low-temperature-grown AlAs/GaAs superlattices experience pronounced interface intermixing with increasing anneal temperatures up to 900 °C. Quantum confinement shifts caused by intermixing of low-temperature-grown and standard-temperature-grown superlattices were studied using electromodulation spectroscopy. The effective activation energy for intermixing in the low-temperature-grown superlattices during 30 s isochronal postgrowth anneals was found to be (0.32 ± 0.04) eV, anomalously smaller than for standard-temperature-grown superlattices. Roughening of the interfaces caused by arsenic precipitates accompanies the intermixing. Qualitative features of the intermixing have been confirmed using high resolution transmission electron microscopy and studies on x-ray rocking curves. © *1995 American Institute of Physics.*

With the advent and extensive development of molecular beam epitaxy (MBE) and metalorganic chemical vapor deposition (MOCVD), the growth of superlattices and abrupt heterojunctions has become commonplace. High-speed transistors and optoelectronic devices depend critically on the abrupt nature of these heterojunctions. The optical and electrical performance of these devices also depend critically on the structural and morphological properties of the interfaces. As a result, interface intermixing and roughening in superlattices associated with impurity atoms,[1] misorientation effects,[2] inverted interfaces,[3] and annealing conditions[4] have been extensively studied. Several techniques, including chemical mapping,[5] high resolution transmission electron microscopy,[6] x-ray rocking curves,[7] scanning tunneling microscopy,[8] photoluminescence,[9] and Monte Carlo simulations[10] have been exploited to study the interdiffusion process. Low-temperature-growth (LTG) GaAs has attracted significant recent attention as a marketable new ultrafast subpicosecond photoconductor.[11–13] This ultrafast property would be important for photorefractive,[14] electro-optic sampling,[15] and saturable absorption applications if it could be combined with sharp quantum-confined excitons in multiple quantum wells (MQWs). The recent discovery[16] of simultaneous ultrafast lifetimes and sharp optical transitions of quantum-confined excitons in AlAs/GaAs quantum wells grown at low substrate temperatures has made LTG MQWs an attractive candidate for a host of new applications. These all-semiconductor devices do not require Cr doping nor postgrowth processing such as ion implantation. Narrow barriers of AlAs between the wells and low excess arsenic concentrations make sharp excitons in LTG quantum wells possible. However, high temperature anneals ($\geqslant$700 °C) cause enhanced interdiffusion that roughen the interfaces. We present studies on interface intermixing observed in *undoped* LTG MQWs and calculate the effective activation energy for intermixing in LTG MQWs.

Two different growths were investigated. The first growth used in our experiments was LTG MBE AlAs/GaAs MQWs grown using As_4. Contact and stop-etch layers of *n*-type materials were grown on a n^+ GaAs substrate at 600 °C. This was followed by LTG (310 °C) MQW layers consisting of a 150 period superlattice of 100 Å GaAs wells and 35 Å AlAs barriers. A 2000 Å *p*-$Al_{0.3}Ga_{0.7}As$ (1×10^{18} cm^{-3}) layer followed by a 2000 Å top *p*-GaAs (1×10^{19} cm^{-3}) layer were grown at 450 °C on top of the LTG layers. The 450 °C growth temperature for the *p*-doped layers acts as a weak *in situ* anneal of the previously grown LTG layers and results in the formation of As precipitates in the MQW region.[17,18] The arsenic clusters deplete free carriers from the surrounding material, rendering it high resistivity.[19] The second growth was identical in all respects except the entire structure was grown at standard temperatures (600 °C), which will henceforth be referred to as standard temperature grown (STG). Appropriate mesas and gold contacts were made to the top *p*-GaAs. The samples were epoxied to glass to remove the substrate using standard techniques. Another gold contact was made to the exposed *n*-$Al_{0.5}Ga_{0.5}As$ stop-etch layer after substrate removal. Electro-optic characterization was performed on the *p-i-n* transmission modulators using a monochromator and an incoherent tungsten lamp.

Both growths were subjected to rapid thermal anneal at several temperatures (up to 900 °C) for 30 s. The rapid thermal anneal in the LTG samples controls the size and spacing of the As precipitates utilizing precipitate engineering.[18] The process of annealing, which forms As clusters, converts LTG GaAs into a high-quality GaAs matrix. Therefore, sharper excitonic features are normally observed for higher anneal temperatures as the LTG material approaches stoichiometric GaAs. In our absorption spectra, we observe the opposite

[a]Electronic mail: lahiri@physics.purdue.edu

 0003-6951/95/67(9)/1244/3/$6.00

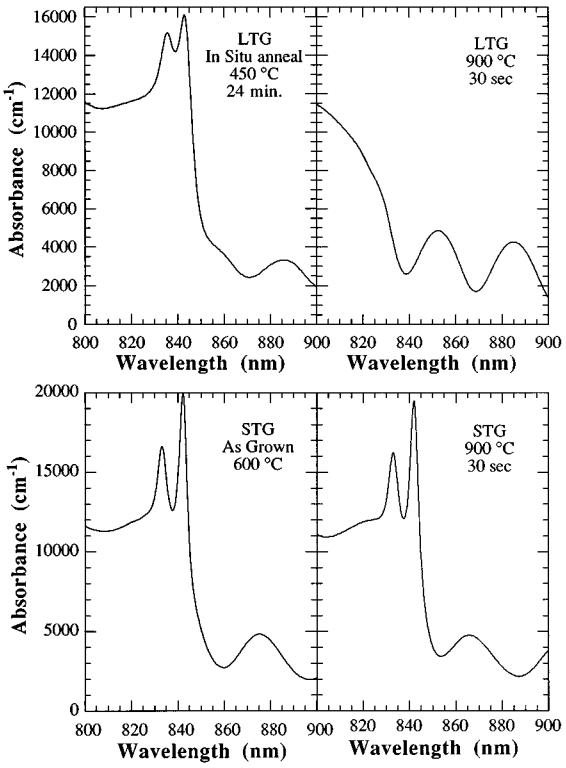

FIG. 1. Absorption spectra for low-temperature-grown (LTG) and standard-temperature-grown (STG) samples, as-grown and with a 900 °C anneal. The sharp quantum-confined excitons are significantly broadened in the LTG samples annealed at 900 °C.

trend.[16] Our sample with the *in situ* anneal of 24 min at 450 °C during the growth of the top 2000 Å *p*-GaAs epilayer gave the sharpest quantum-confined excitons without additional postgrowth anneal. The sharp excitonic features get washed out at higher postgrowth anneal temperatures, caused by interface intermixing. Sharp quantum-confined excitons were observed in all our STG samples irrespective of the anneal conditions.

The zero-field absorbance versus wavelength, for both the LTG and STG as-grown and 900 °C annealed samples, is shown in Fig. 1. Fabry–Perot fringes are evident in the spectra because the samples did not have antireflection coatings. Sharp quantum-confined exciton spectra are observed in both the LTG and STG samples annealed at low temperatures ($\leqslant$700 °C).[16] However, the excitonic features in the LTG samples are washed out for postgrowth anneal temperatures higher than 700 °C. The STG samples, on the other hand, showed no perceptible change under all anneal conditions.

The transition energy of the heavy-hole exciton as a function of anneal temperature for both growths is shown in Fig. 2. The transition energy of the heavy-hole exciton begins to rise for anneal temperatures $\geqslant$700 °C in the LTG samples, indicating a rounding of the wells caused by enhanced interdiffusion. No change in the transition energy was observed for the STG samples, shown in the figure. This points directly towards the role of excess arsenic in the interdiffusion process. Also shown in Fig. 2 is the low-field linewidth Γ as a function of anneal temperature for the LTG samples, measured from the electroabsorption spectra. The

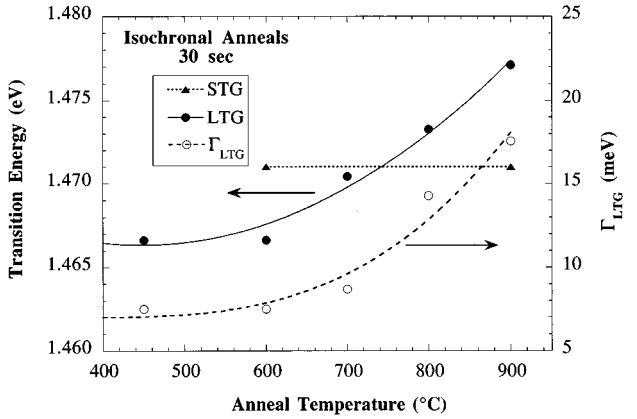

FIG. 2. Exciton transition energy of the heavy-hole exciton vs anneal temperature for the low-temperature-grown (LTG) samples compared with representative data for the as-grown and 900 °C annealed standard-temperature-grown (STG) sample. Also shown is the low-field linewidth Γ vs anneal temperature for the LTG samples.

excitons in the LTG samples broadened from 6 meV for the as-grown samples to 14 meV for the 900 °C annealed samples. Annealing the LTG superlattices therefore produces pronounced intermixing and roughening of the interfaces.

The interdiffusion process was further investigated and confirmed using high resolution transmission electron microscopy (TEM) and studies on x-ray rocking curves. In the (002) x-ray rocking curve, the *in situ* annealed LTG samples have satellites up to order $n=-6$ while the 900 °C annealed LTG samples have satellites only up to $n=-3$. The STG as-grown and the 900 °C annealed samples showed similar x-ray rocking curves with satellite peaks up to order $n=-6$. The details of the TEM measurements and the x-ray rocking curves will be reported in a future publication.

Intermixing of the Al and Ga at the AlAs/GaAs interface causes an increase of the transition energy of the lowest quantum-confined exciton. We can accurately quantify this intermixing by calculating the confinement energy shifts for diffused concentration profiles. The concentration profile $C(x)$ of Al for a given diffusion length L_D is given by the expression

$$C(x)=\frac{bh}{L}-\sum_{n=1}^{\infty}\left(\frac{2h}{n\pi}\right)\sin\left(\frac{n\pi a}{L}\right)\cos\left(\frac{2n\pi x}{L}\right)\times\exp\left(-\frac{4\pi^2n^2L_D^2}{L^2}\right), \tag{1}$$

where b is the barrier thickness, a is the well thickness, and $L=a+b$. The concentration profile defines a potential $V[C(x)]$ and efffective mass $m^*[C(x)]$ obtained from Ref. 20. These functions appear in the Schrödinger equation

$$\nabla^2\psi(x)=\frac{2m^*(x)}{\hbar^2}[V(x)-E]\psi(x) \tag{2}$$

for the interdiffused wells. Equation (2) was solved for the ground state electron and hole energies E using a fourth-order Runge–Kutta algorithm.

The optical transition energy shifts as a function of diffusion length were fit to the experimental data in Fig. 2 to

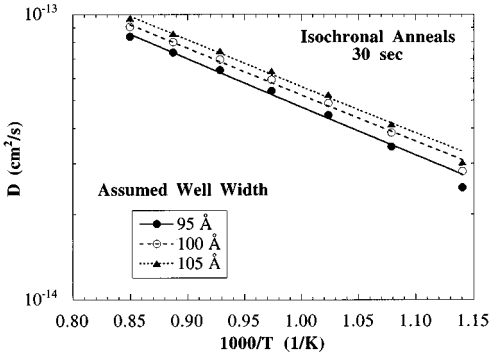

FIG. 3. Diffusion constants for the low-temperature-grown (LTG) samples vs anneal temperature simulated assuming different well widths. The activation energy for intermixing was found to be (0.32 ± 0.04) eV for all three cases.

obtain the diffusion length for a given isochronal anneal temperature. The diffusion constant, shown in Fig. 3 as a function of anneal temperature, was obtained by assuming different well widths to account for the uncertainty of the well widths during MBE growth. The data are fit by exponentials and all yield an effective activation enthalpy $\Delta H_m=(0.32\pm0.04)$ eV for the migration of the Al and Ga ions at the interface. The maximum diffusion length was found to be 5.7 Å for the samples annealed at 900 °C for 30 s. The prefactor fit from the data is $D_0 e^{\Delta S/k_B}=1.6\times10^{-18}$ m^2/s.

Our measured migration energy is significantly smaller than values for migration enthalpy for interdiffusion of AlAs/GaAs quantum wells grown at standard temperatures. A recent study using chemical mapping in electron microscopy studies obtained a value for the migration enthalpy of $\Delta H_m=1.7$ eV.[21] This value was attributed to the migration enthalpy for gallium vacancy diffusion. Our value is considerably smaller than this. The anomalously small value that we obtain for the LTG quantum wells is made plausible by values measured for the annealing of nonphotoquenchable arsenic antisites in LTG GaAs. The migration enthalpy for these defects is $\Delta H_m=(1.1\pm0.3)$ eV,[22] considerably smaller than for gallium vacancies. In addition, the activation enthalpy for arsenic precipitate coarsening in LTG GaAs was found to be 0.87 eV.[23] In both cases it has been conjectured that the excess arsenic in LTG materials lowers the diffusion barriers. However, our value of 0.32 eV is anomalously small compared to all these values, which suggests a strong nonequilibrium diffusion mechanism for interface intermixing in which the diffusion constant is time dependent. Therefore, the excess arsenic in the LTG quantum well structures appears to play a fundamental role for AlAs–GaAs interdiffusion. Extensive reviews address the role of point defects and diffusion mechanisms in GaAs.[1,24] However, the role of excess arsenic in semi-insulating LTG MQWs in the interdiffusion process has not previously been addressed.

In conclusion, we have observed pronounced intermixing and roughening of the AlAs–GaAs interfaces in low-temperature-grown superlattices subjected to high-temperature isochronal anneals with significantly smaller migration energies than observed for standard-temperature-grown superlattices. The excess arsenic in these materials appears to provide a mechanism for strong nonequilibrium interdiffusion, but further work will be required to establish the exact details of the microscopic mechanism. The interdiffusion of these superlattices can play both a detrimental role as well as a beneficial role for applications. For instance, interdiffusion and roughening broadens the excitonic transitions, making them less useful for electro-optic and nonlinear optical applications. On the other hand, impurity-induced superlattice intermixing is commonly used as a technique to fabricate planar waveguides in semiconductors. Therefore, one goal of future research would be to find if the interdiffusion mechanism can be controlled to either enhance or diminish the effect as needed.

Helpful discussions with W. Walukiewicz are gratefully acknowledged. This work was supported in part by the MRSEC Program of the National Science Foundation under Award No. DMR-9400415. D. D. Nolte also acknowledges support by the NSF Presidential Young Investigator program. M. R. Melloch also acknowledges support from the U.S. Air Force Office of Scientific Research under Grant No. F49620-93-1-0031.

[1] D. G. Deppe and N. Holonyak, J. Appl. Phys. **64,** R93 (1988).
[2] M. Tanaka and H. Sakaki, J. Appl. Phys. **64**, 4503 (1988).
[3] F. Alexandre, J. L. Lievin, M. H. Meynadier, and C. Delalande, Surf. Sci. **168**, 454 (1986).
[4] B. Elman, E. S. Koteles, P. Melman, and C.A. Armiento, J. Appl. Phys. **66**, 2104 (1989).
[5] A. Ourmazd, D. W. Taylor, J. Cunningham, and C. W. Tu, Phys. Rev. Lett. **62**, 933 (1989).
[6] A. F. DeJong, H. Bender, and W. Coene, Ultramicroscopy **21**, 373 (1987).
[7] R. M. Fleming, D. B. McWhan, A. C. Gossard, W. Wiegmann, and R. A. Logan, J. Appl. Phys. **51**, 357 (1980).
[8] R. M. Feenstra, D. A. Collins, D. Z. Y. Ting, M. W. Wang, and T. C. McGill, Phys. Rev. Lett. **72**, 2749 (1994).
[9] C. Delalande, Surf. Sci. **168**, 531 (1986).
[10] J. Singh and K. K. Bajaj, Appl. Phys. Lett. **47**, 594 (1985).
[11] F. W. Smith, H. Q. Le, V. Diadiuk, M. A. Hollis, A. R. Calawa, S. Gupta, M. Frankel, D. R. Dykaar, G. A. Mourou, and T. Y. Hsiang, Appl. Phys. Lett. **54**, 890 (1989).
[12] B. C. Tousley, S. M. Mehta, A. I. Lobad, P. J. Rodney, P. M. Fauchet, and P. Cooke, J. Electron. Mater. **22**, 1477 (1993).
[13] E. S. Harmon, M. R. Melloch, J. M. Woodall, D. D. Nolte, N. Otsuka, and C. L. Chang, Appl. Phys. Lett. **63**, 2248 (1993).
[14] *Photorefractive Effects and Materials*, edited by D. D. Nolte (Kluwer Academic, Dordrecht, 1995).
[15] W. H. Knox, J. E. Henry, K. W. Goossen, K. D. Li, B. Tell, D. A. B. Miller, D. S. Chemla, A. C. Gossard, J. English, and S. Schmitt-Rink, IEEE J. Quantum Electron. **25**, 2586 (1989).
[16] I. Lahiri, D. D. Nolte, E. S. Harmon, M. R. Melloch, and J. M. Woodall, Appl. Phys. Lett. **66**, 2519 (1995).
[17] M. R. Melloch, N. Otsuka, J. M. Woodall, A. C. Warren, and J. L. Freeouf, Appl. Phys. Lett. **57**, 1531 (1990).
[18] M. R. Melloch, J. M. Woodall, N. Otsuka, K. Mahalingam, C. L. Chang, D. D. Nolte, and G. D. Pettit, Mater. Sci. Eng. B **22**, 31 (1993).
[19] A. C. Warren, J. M. Woodall, P. D. Kirchner, X. Yin F. Pollak, M. R. Melloch, N. Otsuka, and K. Mahalingam, Phys. Rev. B **41**, 4617 (1992).
[20] S. Adachi, J. Appl. Phys. **58**, R1 (1985).
[21] J.-L. Roviere, Y. Kim, J. Cunningham, J. A. Rentschler, A. Bourret, and A. Ourmazd, Phys. Rev. Lett. **68**, 2798 (1992).
[22] D. E. Bliss, W. Walukiewicz, and E. E. Haller, J. Electron. Mater. **22**, 1401 (1993).
[23] K. Mahalingham, N. Otsuka, M. R. Melloch, J. M. Woodall, and A. C. Warren, J. Vac. Sci. Technol. B **9**, 2328 (1991).
[24] T. Y. Tan, U. Gösele, and S. Yu, Crit. Rev. Solid State Mater. Sci. **17**, 47 (1991).